Patterned 3D-printed hydrogel as a novel soilless substrate for plant cultivation

Ali Mohammed[2,3†], Maddalena Salvalaio[1†], Yumeng Li[2], Connor Myant[2], Giovanni Sena[1*]

† *These authors contributed equally to this work*
* *Corresponding author: g.sena@imperial.ac.uk*

1. *Department of Life Sciences, Imperial College London, London SW7 2AZ, UK*
2. *Dyson School of Design Engineering, Imperial College London, SW7 2AZ, UK*
3. *School of Design, Royal College of Art, SW11 4AY London, U.K.*

ABSTRACT

Plant roots need water, micronutrients, and oxygen to maintain cellular metabolism and tissue growth, yet traditional hydroponic systems often lack sufficient oxygen delivery. While 3D printing artificial substrates has been explored to mimic the physical structure of soil, it remains unclear which design parameters are critical for supporting full plant development. Here, we present a synthetic, soilless substrate based on 3D-printed hydrogels incorporating triply periodic minimal surface (TPMS) patterns to create internal air-filled channels. These channels remain in contact with the atmosphere, enabling passive gas exchange throughout the substrate.

We tested five TPMS geometries (Lidinoid, Split-P, Schwarz-D, Schwarz-P, and Schoen), each with an identical hydrogel volume but with different surface-to-volume ratios. Arabidopsis thaliana seeds germinated directly on the substrates and were monitored for vegetative and reproductive growth over five weeks. Among the designs, the Lidinoid substrate consistently led to the highest number and size of leaves and the earliest and most complete flowering, outperforming both hydroponics and unpatterned hydrogel controls.

Our results indicate that the surface-to-volume ratio is a key parameter influencing substrate performance, likely due to its impact on oxygen availability at the root interface. Plants grown on substrates with higher surface areas transitioned to flowering more reliably and rapidly, with flowering efficiency showing a strong positive correlation with surface area. These findings suggest that vascular-like internal architectures can overcome the oxygen limitations of traditional hydroponic systems without requiring active aeration.

This work supports the use of additive manufacturing as a powerful tool for engineering soil analogues tailored for indoor agriculture. By combining passive aeration with hydration and nutrient delivery, patterned hydrogels offer a promising, scalable solution for sustainable soilless plant cultivation.

BACKGROUND

Land plants rely on their root system for water and micronutrient uptake from soil. Root cells depend on oxygen for aerobic cellular respiration, which provides energy in the form of ATP for the cellular physiological processes driving growth and maintenance of biomass, and uptake and maintenance of intracellular ions [1,2]. Consequently, soil oxygenation, or more broadly aeration, is a crucial factor when considering root-soil interaction and the extent of life support offered by a type of soil.

Roots growing in conditions providing sub-optimal (hypoxia) or undetectable (anoxia) oxygen concentration experience a diminished aerobic metabolism with reduced ATP production [3]. Although some plants evolved defence physiological mechanisms to deal with this type of abiotic stress [4], extensive exposure to hypoxia and anoxia leads to severe cellular damage and physiological perturbations linked to cell acidification and the accumulation of reactive oxygen species (ROS) and reactive nitrogen species (RNS) [5,6].

In soil, oxygen can be found dissolved at relatively low concentrations in water and much higher concentrations in paths or pockets of air. The oxygen diffusion rate is also higher in air than in water, making passive oxygen uptake more efficient from air pockets than from water.

Cellular respiration rates in roots vary with plant species, root region [7]), and environmental conditions [1]. Since oxygen is poorly soluble in water (Henry's constant of gaseous vs. aqueous concentration of O_2 at 25 °C and 1 atm is 31.46 [1]), the content of oxygen in soil is dominated by its gaseous phase in air pockets. The amount of air in soil (soil aeration) mainly depends on diffusion from the atmosphere through open passages in soil [8]. In essence, soil aeration depends on its macroscopic geometry, which can be described by quantities such as porosity (bulk density), particle size distribution (soil texture), pore size distribution, and connectivity of the pore network (coordination number) [1]. This is the main reason soil compaction reduces root growth and plant biomass, as indicated by a strong correlation between poor soil aeration and crop yield [9,10].

In modern agriculture, several methods have been adopted to increase soil aeration, with mixed results: tillage (e.g. ploughing), air injection, irrigation with water containing air bubbles or hydrogen peroxide, and even the mixing of solid peroxides to soil [1]. More recently, the increasing requirement for more efficient and sustainable food production, together with a need to minimise water and land use, is pushing the development of soil-less cultivation methods to be used in indoor and vertical farming. Although liquid (hydroponics and aquaponics solutions) and mist (aeroponics) media can be used to grow small crops [11], the infrastructure and energy consumption required to run and maintain these systems are often complex and expensive, reducing their commercial and ecological sustainability. Alternative methods are required to reach a higher level of production and sustainability [12].

Is it possible, instead, to manufacture a soil-less substrate to deliver water, nutrients, and oxygen to plant roots in a passive way (*i.e.,* without pumps)? The idea of producing a solid substrate that resembles some of the geometrical and mechanical properties of soil, and potentially aeration by diffusion, is not new. A simple approach is to cluster solid fragments randomly, such as in the "transparent soil" made of clear gel [13] or other polymers [14]. More complex structures have been proposed, based on wet granular medium [15] or built with additive manufacturing (3D printing) with hydrogels [16–19] or other material. In some cases, the 3D-printed structure has been explicitly designed to resemble some of the geometrical traits of real soil [20,21]. In fact, although hydrogels have been 3D-printed in the past using various methods and chemical compositions, not all printable solutions are non-toxic and biocompatible [22].

Overall, these and other results suggest that hydrogel can be adopted as a substrate for plant culture [23] and that a solid substrate can be designed and manufactured to mimic some of the key properties of soil. It has recently been shown that 3D-printed porous substrates made of hydrogel result in increased root growth in some plant species when compared to a non-porous hydrogel substrate [19]. Although this is a significant step forward toward the realisation of a 3D-printed substrate for plants, a demonstration that the passive aeration in these designs is sufficient to support a sustained and robust plant growth in comparison to traditional hydroponics is, to our knowledge, still missing.

We present a novel method for designing, optimising, and 3D printing high-resolution triply periodic minimal surface (TPMSs) hydrogels with interconnected channel networks that remain in contact with the atmosphere. We show that the plant model system *Arabidopsis thaliana* can germinate, grow, and flower on the 3D-printed hydrogel substrates, with its root system extending on the inner surface of the channels. We compare the performance of various TPMSs network topologies by quantifying average leaf size, leaf number, and flowering times in Arabidopsis plants.

METHODS

Hydrogel material

The following reagents were purchased from Sigma-Aldrich (Dorset, UK) unless stated otherwise: acrylamide (AAm; ≥ 99%), poly (ethylene glycol) diacrylate (PEGDA 700; average Mn 700), lithium phenyl-2,4,6-trimethylbenzoylphosphinate (LAP; ≥ 95%), 1-phenylazo-2-naphthol-6,8-disulfonic acid disodium salt (Orange G), Glycerol for molecular biology ≥99.0%

(G5516), Murashige and Skoog (MS) plant growth medium MS Basal medium (M5519), MES hydrate (M8250) and Tris buffer (Fisher-Scientific, 10205100).

CAD design

A MATLAB code was developed to create a series of Triply Periodic Minimal Surfaces (TPMSs) CAD models with varying surface area-to-volume ratios. The 5 chosen designs to explore were Lidinoid, Split-P, Schwarz-D, Schoen and Schwarz-P. A hydrogel volume fraction of 0.6 was selected for all designs, based on printability, sufficient volume to maintain internal void structures without becoming solid, and adequate thickness for the structure to support itself once printed. The MATLAB models were converted into STL files compatible with the SLA printer used in this work. All CAD models were 2x2x2 cm^3. A control solid structure with a volume fraction of 1 was used as a control standard against the 5 structures.

Photo-resin preparation

The photo-resin was prepared based on a final total volume of 100 g. In order of mixing, 5% (w/w) $PEGDA_{700}$ cross-linker, 15% (w/w) AAm monomer and 5% (w/w) glycerol softening agent were added to a clean 150 ml amber bottle. 80 g of deionised water was added to the mixture and left to stir using a magnetic stirring plate for 30 min until fully dissolved. Next, relative to the total mass of monomer and cross-linker, 1% LAP and 0.24% Orange G were added to the mixture and left to stir for another 30 min until fully dissolved. The pH of the final photo-resin was adjusted to 5.7 using Tris buffer and 0.05% (w/v) MES hydrate prior to 3D printing.

3D printing

The final formulation was poured into a Formlabs Resin LT Tank and plugged into a Form 2 SLA printer (Formlabs, 405 nm light source, 140 µm laser spot size). 'Open Mode' setting was used which allows for use of 3rd party photo-resins. CAD models were uploaded using the Preform software with 'Clear Resin V4' settings, 100 µm layer height and no support structures. During the printing process, the print was paused every 10 layers to carefully remove any bubbles formed in the photo-resin due to the surface tension between the build plate and the tank.

Once the print was complete, the build platform was carefully detached from the printer, and printed substrates were immediately rinsed with DI water whilst attached to the platform to ensure excess photo-resin is removed. 3D-printed samples were then detached using a thin string and placed into a clear pot filled with DI water. The DI water was replaced twice to ensure that excess photo-resin is removed within the network of channels of the hydrogels. Once fully cleaned, the DI-water was replaced again, and the hydrogels were post-cured for 8 min using a FormCure (Formlabs) post-curing station with a 405 nm light source to photo-

cure any unreacted monomers and cross-linkers.

Dehydration and rehydration

The 3D-printed hydrogels were dehydrated in open air at room temperature for 24 hours. Once dehydrated, the hydrogels were then soaked in ¼ Murashige and Skoog (MS) plant growth medium: 0.1075% (w/v) MS basal medium, 0.05% (w/v) MES hydrate, pH adjusted to 5.7 with Tris buffer to allow the hydrogels to absorb the nutrients necessary for plant growth. The soaking medium was discarded and replaced with fresh ¼ MS medium daily for 7 days, to remove from the hydrogel any remaining monomers and cross-linkers.

Plant material

Wild-type *Arabidopsis thaliana* seeds, Columbia (Col-0) ecotype, were used for this work. Seeds were imbibed in water and kept in the dark at 4°C for two days to synchronise germination. Seeds were surface sterilised with 50% (v/v) Haychlor bleach and 0.0005% (v/v) Triton X-100 for 3 min and then rinsed with sterilised Milli-Q water six times. Sterilised seeds were sown on the top surface of each hydrogel print, which were then placed inside Magenta boxes (Sigma-Aldrich, V8380). The boxes were transferred to a growth chamber at 22 °C, with a (16 h : 8 h) = (light : dark) photoperiod and light intensity 120 µmol m^{-2} s^{-1}.

Hydroponics

For the hydroponics control, seeds were sown in PCR tubes containing ¼ MS solid medium (0.1075% (w/v) MS Basal medium, 0.05% (w/v) MES hydrate, 0.8% (w/v) agar (Sigma-Aldrich 05040), pH adjusted to 5.7 with Tris Buffer. The tips of the PCR tubes were cut to allow the growing roots to come out and then were inserted in a 3D-printed support placed inside Magenta boxes (Sigma-Aldrich, V8380) filled with ¼ MS liquid medium, as previously described [24]. A 0.5 µm diffusion stone connected to an air pump was placed inside each Magenta box, to aerate the liquid medium. The Magenta boxes were then transferred to a growth chamber at 22 °C, with a (16 h : 8 h) = (light : dark) photoperiod and light intensity 120 µmol m^{-2} s^{-1}.

Experimental design

For the hydrogel prints, two sterilised *Arabidopsis* seeds were sown on top of each print, and two prints were placed in each Magenta box; five Magenta boxes were used for each hydrogel design. For the hydroponics control, one sterilised seed was sown in each PCR tube, and 10 tubes were placed in each Magenta box filled with liquid growth medium; five Magenta boxes were used in hydroponic conditions. The entire pipeline, from 3D printing to phenotyping, is summarised in Supplementary Figure 1.

Growth analysis and flowering time

Arabidopsis seedlings were grown in hydrogel and hydroponics substrates for 1, 2, 3, 4, and 5 weeks. At the end of each week, leaves were cut from the plants with dissecting scissors (Wolflabs 503667) and laid flat on the surface of a ¼ MS agar plate. The leaves were then visualised under a stereo microscope (Nikon SMZ800N), and images were recorded with a Nikon DS-Fi3 camera using Nikon NIS-Elements Imaging software.

The area of the leaves was determined by analysing the pixels in the captured images. For each image, a colour intensity threshold was manually determined, which was used to generate a contour around the leaf area. The threshold was adjusted as needed for the contour to best represent the area. The total leaf area was then calculated and recorded from the number of pixels within the contour. The flowering time and the number of flowering plants were monitored throughout the experiments without disrupting plants' growth, through a viewing window on the Magenta box lids modified with a custom-cut glass slide (VWR MARI1100420).

Statistical analysis

The statistical analysis on leaf number and area data was done by comparing the 6 different hydrogel designs first, and then the hydroponics control versus each hydrogel design. The normality of the samples was checked with the Shapiro-Wilk test with alpha-level = 0.05. Levene's test with alpha-level = 0.05 was used to assess the equality of variances. For the comparisons among the hydrogel designs, if the distributions were normally distributed and the variances were equal, one-way ANOVA at the 0.05 level with Tukey's multiple comparison test was used. For non-normally distributed data and/or unequal variances among the groups, Kruskal-Wallis ANOVA at the 0.05 level with Dunn's test was performed. For the comparison between each hydrogel design and the hydroponics control, when the samples were normally distributed, the two-sample *t*-test with Bonferroni's correction was used. If one of the distributions was not normal, the Mann-Whitney test with Bonferroni's correction was used. Following Bonferroni-s correction, the alpha level for the two-sample *t*-test and Mann-Whitney test=0.008. All statistical tests were performed with Origin Pro.

In the figures, $*P < 0.05$, $**P < 0.01$, and $***P < 0.001$ in comparisons among hydrogel designs, $*P < 0.008$, $**P < 0.002$, and $***P < 0.0002$ in comparison between hydroponics vs hydrogel designs.

RESULTS

A new growth substrate

In this work, we developed a synthetic hydrogel system that incorporates a growth medium traditionally used for hydroponic cultivation of *Arabidopsis*, along with a periodic network of internal channels connected to the surface to facilitate air circulation for gas exchange. The mechanical impedance of the gel was chosen to induce the plant roots to grow in the channels without penetrating the hydrogel volume. We reasoned that this configuration would allow the roots to uptake water and nutrients from the hydrogel medium and, at the same time, avoid hypoxia by being exposed to oxygen at atmospheric concentrations. Crucially, the water-based hydrogel formulation was developed for additive manufacturing (3D printing), following a method we had previously established to consistently reproduce CAD-designed channels in the final substrate [18].

The hydrogel growth substrates are non-toxic following the process of washing, post-curing, hydration and dehydration, which ensures unreacted chemical components are either photo-cured and/or washed out. Further, after dehydration and hydration, the hydrogels have a buffer pH of 5.7, and contain sufficient micronutrients to support the germination of Arabidopsis seeds placed on their surface and the subsequent plant growth to flowering. The mechanical and chemical properties of our hydrogel system have been previously optimised for high-resolution 3D-printing in our previous work [18].

Among the 3D-printable designs that provide interconnected patterns, we focused on a class of Triply Periodic Minimal Surfaces (TPMS) defined by high surface-area-to-volume ratios (SA/V) and composed of infinite, non-self-intersecting, and periodic surfaces in three principal directions [25,26]. The core idea was to mimic biological structures in which high SA/V ratios enhance gas or nutrient exchange, ensuring adequate oxygenation for the root system. A second important parameter is how much of the whole substrate is made of hydrogel, or Hydrogel Fraction (HF). For simplicity, we normalised SA/V to the control case of a cubic substrate with no channels (we call it “solid”), defined with SA/V=1 and HF=1.

We identified 5 candidate TPMS patterns that, in principle, could be realised across a range of SA/V vs HF (Fig. 1): Lidinoid, Split P, Schwarz D, Schwarz P, Schoen [26,27]. In practice, spatial resolution limitations in the 3D printing method and structural constraints to prevent the substrate from collapsing under its own weight or simply to sustain mechanical stress during handling, we limited our study to realisations with HF=0.6.

Two *Arabidopsis* seeds were sterilised and placed on top of each 3D-printed substrate. Plantlets were left on the same substrate and grown for 1 to 5 weeks after sowing. One control was constituted by a “solid” substrate, 3D-printed with the same hydrogel

composition but without channels. A traditional liquid culture (hydroponics) containing the same concentration of micronutrients used in the hydrogel was adopted as a second control representing the traditional hydroponic cultivation currently mostly popular in soilless indoor farming.

To compare the effectiveness of the network designs among themselves and with traditional hydroponics, we selected three developmental traits to measure for successful plant growth: leaf number, leaf area and flowering time.

Leaf number

To quantify vegetative growth, we focused on leaf development and first counted the leaf number on each plant growing on a 3D-printed substrate at the end of every week.

After the first week, the two cotyledons (embryonic leaves) emerged from all the plants grown in the five substrates and the hydroponics (Fig. 2 a). A few plants grew true leaves in the Lidinoid, but also in the solid substrate and hydroponics; plants grown in the Lidinoid substrate developed an average of 2.8 leaves per plant, showing the best yield among all the designs (Fig. 2 a, Dunn's test between Lidinoid and Schoen, Lidinoid and Schwarz-D, Lidinoid and Schwarz-P, Lidinoid and Split-P, P=0.018).

After 2 weeks, plants grown in Split-P, solid, and hydroponics still had only the two cotyledons, while all the other designs developed non-embryonic leaves as well (Fig. 2 b). Among these, Lidinoid, Schwarz-D and Schoen were more efficient in leaf number development than the solid hydrogel (Fig. 2 b, Dunn's test between solid and Lidinoid, and solid and Schwarz-D , P<0.001; Dunn's test between solid and Schoen, P<0.05) and the hydroponics control (Mann-Whitney test with Bonferroni correction between hydroponics and Lidinoid, P= 0.001, hydroponics vs Schoen, and hydroponics vs Schwarz-D, P<0.008).

In the subsequent weeks, the number of leaves developed by plants grown in the Lidinoid substrate was always greater than those grown in the solid hydrogel (see Supplementary Table 1 for detailed statistics). After four weeks, Lidinoid, Schoen, Schwarz-D, Schwarz-P and Split-P all generated more leaves than the solid hydrogel (Fig. 2 d, Tukey test, solid vs Lidinoid, solid vs Schoen, solid vs Schwarz-D, solid vs Schwarz-P, solid vs Split-P, P<0.001).

A statistically significant difference between the number of leaves developed in any patterned hydrogel and hydroponics was observed only at week 2 (Fig. 2 b). This might be due to the unusually large variability in leaf number in plants grown in hydroponics (Fig. 2 c, d, and e). Moreover, when plotting the number of emerged leaves as a function of time (Fig. 2 f), it appears that the rate of leaf production was higher for plants grown in patterned hydrogels, compared to those grown in solid hydrogel or hydroponics.

Leaf area

To further quantify the effect of patterned hydrogel substrate on shoot growth, we also measured the average leaf size in each plant and compared those grown on patterned substrates to those grown in solid hydrogel or hydroponics. Briefly, all leaves were cut from each plant weekly, and their area was individually measured with the aid of a dissecting microscope and Image-J (see Methods).

After only one week, Lidinoid was the patterned substrate where plants developed the largest average leaf size (Fig. 3 a, see Supplementary Tables 3 and 4 for detailed statistics). Moreover, in the first week, plants in all patterned hydrogels showed an average leaf area larger than that of the hydroponics control (Fig. 3 a, see Supplementary Table 4 for detailed statistics).

After two weeks, plants grown in Lidinoid, Schoen, and Schwarz-D developed leaves bigger than those grown on the solid hydrogel (Fig. 3 b, Dunn's test between solid and Lidinoid, $P<0.001$, solid and Schoen, $P=0.014$, solid and Schwarz-D, $P<0.01$) and the hydroponics control (Fig. 3 b, two-sample *t*-test with Bonferroni correction between hydroponics and Lidinoid, $P<0.0002$, hydroponics vs Schoen and hydroponics vs Schwarz-D, $P<0.002$).

After three and four weeks, all the plants on patterned hydrogels on average had larger leaves than those on the solid hydrogel (Fig. 3 c, and d, see Supplementary Table 3 for detailed statistics), corroborating the results on leaf number at week 4 (Fig. 2 d). During the first four weeks, the Lidinoid design performed consistently better in leaf size compared to the traditional hydroponics (Fig. 3 a-d and Table 4 for detailed statistics). However, the statistical significance was lost during week 5, probably due to the substantial variability among plants grown in the Lidinoid (Fig. 3 e). In fact, after five weeks, the three plants that developed the biggest average leaf area of all (38.3, 40.2, and 43.9 mm^2) were all grown in the Lidinoid hydrogels (Fig. 3 e). Furthermore, the plot of average leaf area as a function of time (Fig. 3 f) indicates that the plants growing on the Lidinoid were the ones with the highest rate of leaf growth, while the ones growing in solid hydrogel or hydroponics were the ones with the lowest rate.

Finally, except for week 1 (Fig 3. a, two-sample *t*-test with Bonferroni correction between hydroponics and solid, $P<0.0002$), the solid hydrogel and the hydroponics substrates were always indistinguishable from each other both in leaf number and average leaf area (see Supplementary Tables 1, 2,3, and 4 for detailed statistics).

Flowering

Besides assessing vegetative growth with leaf development, we also analysed reproductive growth by quantifying the time required to develop the first flowers, or flowering time. Strikingly,

plants grown in Lidinoid, Schoen, Schwarz-D and Split-P patterned hydrogels produced flowers within five weeks (35 days) after sowing, while plants grown in Schwarz-P, solid hydrogels and hydroponics did not (Fig. 4). The first flowering event took place in the Lidinoid hydrogel on day 25, followed by Split-P on day 26 and Schoen and Schwarz-D on day 28 (Fig. 4). By the end of the five weeks, 100% (± 13.4% s.e.p.) of the plants grown in Lidinoid flowered, while only 60% (± 9.5% s.e.p.) of plants in Split-P, 30% (± 12.7% s.e.p.) in Schwarz-D and 10% (± 9.5% s.e.p.) in Schoen hydrogels flowered (Fig. 4). Plants in the Lidinoid hydrogel were the fastest to reach the vegetative-reproductive developmental transition, with all plants flowering after only four weeks (Fig. 4).

Interestingly, when considering the total percentage of flowered plants, the performance of each design is positively correlated to the normalised surface area (Fig. 5), i.e. with a higher surface area corresponding to a higher % of flowering plants at day 35.

DISCUSSION

The idea of 3D printing an artificial substrate to replicate some of the physical and topological traits of natural soil is not entirely new [19–21]. What remains less clear is which of these traits suffice to support the long-term and robust growth of an entire plant. More specifically, what is the minimal design and composition required to create an artificial substrate on which a flowering plant can germinate and grow leaves and flowers?

In this work, we show that a block of hydrogel, patterned with an internal periodic network of air-filled tubules, is sufficient to sustain germination, vegetative growth, and flowering in the model plant *Arabidopsis thaliana*. Moreover, we show that the specific geometry of the periodic tubule network significantly influences plant growth.

Among the TPMS patterns tested, the Lidinoid design consistently outperformed the others in terms of average number (Fig. 2) and size (Fig. 3) of leaves, as well as flowering time (Fig. 4). Notably, this design offers the highest surface-to-volume ratio among all tested geometries, given the constant hydrogel volume fraction across designs. This outcome is perhaps expected, as a higher surface-to-volume ratio likely improves gas exchange between the water in the hydrogel and the air within the tubule network. It is well established that one limitation of hydroponic (i.e. liquid-based) cultivation is the relatively low concentration of dissolved oxygen in water. Roots require oxygen for cellular respiration, particularly during active growth phases supporting leaf and flower development. The 3D printed substrate described here can be thought of as a “vascularised” hydrogel, with the tubule network facilitating passive diffusion to enhance oxygen availability.

One of the more striking results in this work is that the vascularised hydrogel outperforms a traditional hydroponic substrate in promoting leaf number and size (Fig. 2 and 3), particularly

when using the Lidinoid design. This is further supported by the observation that an unpatterned hydrogel block performs comparably to hydroponics, indicating that it is the geometry of the internal network—rather than the hydrogel material itself—that drives the difference.

Another noteworthy finding is the accelerated leaf growth rate observed with the Lidinoid design, which exceeds that of all other tested geometries and clearly outpaces hydroponic cultivation (Fig. 3 f), reinforcing the conclusion that improved oxygenation enhances vegetative growth.

Finally, we argue that quantitative data on flowering provide a critical metric for evaluating substrate functionality. The ability to transition efficiently from vegetative growth to flowering is a key determinant of plant fitness and has direct implications for fruit production, an important consideration in agritech applications such as indoor crop cultivation. Our results show that the Lidinoid design once again performs best in promoting early flowering (Fig. 4). Notably, flowering efficiency (defined here as the percentage of plants flowering by day 35) correlates strongly with the substrate's surface-to-volume ratio (Fig. 5), further supporting the hypothesis that gas exchange within the tubule network is the driving factor.

Taken together, our findings support a broader strategy of using additive manufacturing (3D printing) as a powerful and scalable method for fabricating finely patterned hydrogels for indoor plant cultivation. While the hydrogel component provides water and micronutrients, the "vascular" tubule network delivers air to oxygen-demanding root meristems. How different is this approach from the way natural soil functions as an optimal substrate for plant growth? We would argue: not very, although a direct comparison lies beyond the scope of this study.

DECLARATIONS

Availability of data and materials

The datasets generated and analysed during the current study are available from the corresponding author on reasonable request.

Competing interests

The authors declare that they have no competing interests.

Authors' contributions

AM and MS contributed equally, developing the methods and conducting most of the experimental work. YL assisted with 3D printing and phenotypic analysis. CM designed the vasculature patterns and provided expertise in 3D printing, while GS contributed plant and biophysics expertise for concept development and phenotyping. CM and GS jointly conceived and coordinated the study. AM, MS and GS drafted the manuscript. All authors read and approved the final version.

Funding

This work was partially supported by two UKRI Impact Acceleration Awards (IAA) (EP/X52556X/1 and BB/S506667/1) and an Imperial's President's Excellence Fund for Frontier Research (EFFR) award.

Acknowledgements

We would like to thank Dr Borut Lampret for helping with code development and analysis tools, and Dr Livia Kalossaka for their assistance during the early development of this study.

REFERENCES

1. Ben-Noah I, Friedman SP. Review and Evaluation of Root Respiration and of Natural and Agricultural Processes of Soil Aeration. Vadose Zone J. 2018;17:1–47.

2. Amthor JS. The McCree–de Wit–Penning de Vries–Thornley Respiration Paradigms: 30 Years Later. Ann Bot. 2000;86:1–20.

3. Arru L, Fornaciari S, Mancuso S. New Insights into the Metabolic and Molecular Mechanism of Plant Response to Anaerobiosis. Int Rev Cell Mol Biol. 2014;311:231–64.

4. Nakamura M, Noguchi K. Tolerant mechanisms to O2 deficiency under submergence conditions in plants. J Plant Res. 2020;133:343–71.

5. Drew MC. Oxygen deficiency and root metabolism: Injury and Acclimation Under Hypoxia and Anoxia. Annu. Rev. Plant Physiol. Plant Mol. Biol. 1997;48:223–50.

6. Hebelstrup KH, Møller IM. Reactive Oxygen and Nitrogen Species Signaling and Communication in Plants. Signal Commun. Plants. 2014;63–77.

7. Mancuso S, Boselli M. Characterisation of the oxygen fluxes in the division, elongation and mature zones of Vitis roots: influence of oxygen availability.Planta. 2002;214:767–74.

8. King FH. Contributions to Our Knowledge of the Aeration of Soils.Science.1905;22:495–9.

9. Gliński J, Stępniewski W. Soil Aeration and Its Role for Plants. 2018.

10. Holtman WL, Oppedijk BJ, Vennik M, Duijn B van. Low-Oxygen Stress in Plants, Oxygen Sensing and Adaptive Responses to Hypoxia. Plant Cell Monogr. 2013;371–80.

11. A. A. Hydroponics, Aeroponic and Aquaponic as Compared with Conventional Farming. American Scientific Research Journal for Engineering, Technology, and Sciences. 2017; 27:247–55.

12. Barrett GE, Alexander PD, Robinson JS, Bragg NC. Achieving environmentally sustainable growing media for soilless plant cultivation systems – A review. Sci Hortic. 2016;212:220–34.

13. Ma L, Shi Y, Siemianowski O, Yuan B, Egner TK, Mirnezami SV, et al. Hydrogel-based transparent soils for root phenotyping in vivo. Proc Natl Acad Sci. 2019;116:11063–8.

14. Downie H, Holden N, Otten W, Spiers AJ, Valentine TA, Dupuy LX. Transparent Soil for Imaging the Rhizosphere. PLoS ONE. 2012;7:e44276.

15. Cejas CM, Hough LA, Beaufret R, Castaing J-C, Frétigny C, Dreyfus R. Preferential Root Tropisms in 2D Wet Granular Media with Structural Inhomogeneities. Sci Rep. 2019;9:14195.

16. Benjamin AD, Abbasi R, Owens M, Olsen RJ, Walsh DJ, LeFevre TB, et al. Light-based 3D printing of hydrogels with high-resolution channels. Biomed Phys Eng Express. 2019;5:025035.

17. Chen Z, Zhao D, Liu B, Nian G, Li X, Yin J, et al. 3D Printing of Multifunctional Hydrogels. Adv Funct Mater. 2019;29.

18. Kalossaka LM, Mohammed AA, Sena G, Barter L, Myant C. 3D printing nanocomposite hydrogels with lattice vascular networks using stereolithography. J Mater Res. 2021;36:4249–61.

19. Li J, Xie J, Wu Q, Wu G, Men Y. 3D-printed hydrogel substrates with tailored pore architectures enhance root development and elicit species-specific growth responses. Chem Eng J. 2025;512:162425.

20. Ferro ND, Morari F. From Real Soils to 3D-Printed Soils: Reproduction of Complex Pore Network at the Real Size in a Silty-Loam Soil. Soil Sci Soc Am J. 2015;79:1008–17.

21. Bacher M, Schwen A, Koestel J. Three-Dimensional Printing of Macropore Networks of an Undisturbed Soil Sample. Vadose Zone J. 2015;14:1–10.

22. Kalossaka LM, Sena G, Barter LMC, Myant C. Review: 3D printing hydrogels for the fabrication of soilless cultivation substrates. Appl Mater Today. 2021;24:101088.

23. Ma L, Chai C, Wu W, Qi P, Liu X, Hao J. Hydrogels as the plant culture substrates: A review. Carbohydr Polym. 2023;305:120544.

24. Salvalaio M, Oliver N, Tiknaz D, Schwarze M, Kral N, Kim S-J, et al. Root electrotropism in Arabidopsis does not depend on auxin distribution but requires cytokinin biosynthesis. Plant Physiol. 2022;188:1604–16.

25. Yoo D-J. Advanced porous scaffold design using multi-void triply periodic minimal surface models with high surface area to volume ratios. Int J Precis Eng Manuf. 2014;15:1657–66.

26. Han L, Che S. An Overview of Materials with Triply Periodic Minimal Surfaces and Related Geometry: From Biological Structures to Self-Assembled Systems. Adv Mater. 2018;30:e1705708.

27. Feng J, Fu J, Yao X, He Y. Triply periodic minimal surface (TPMS) porous structures: from multi-scale design, precise additive manufacturing to multidisciplinary applications. Int J Extreme Manuf. 2022;4:022001.

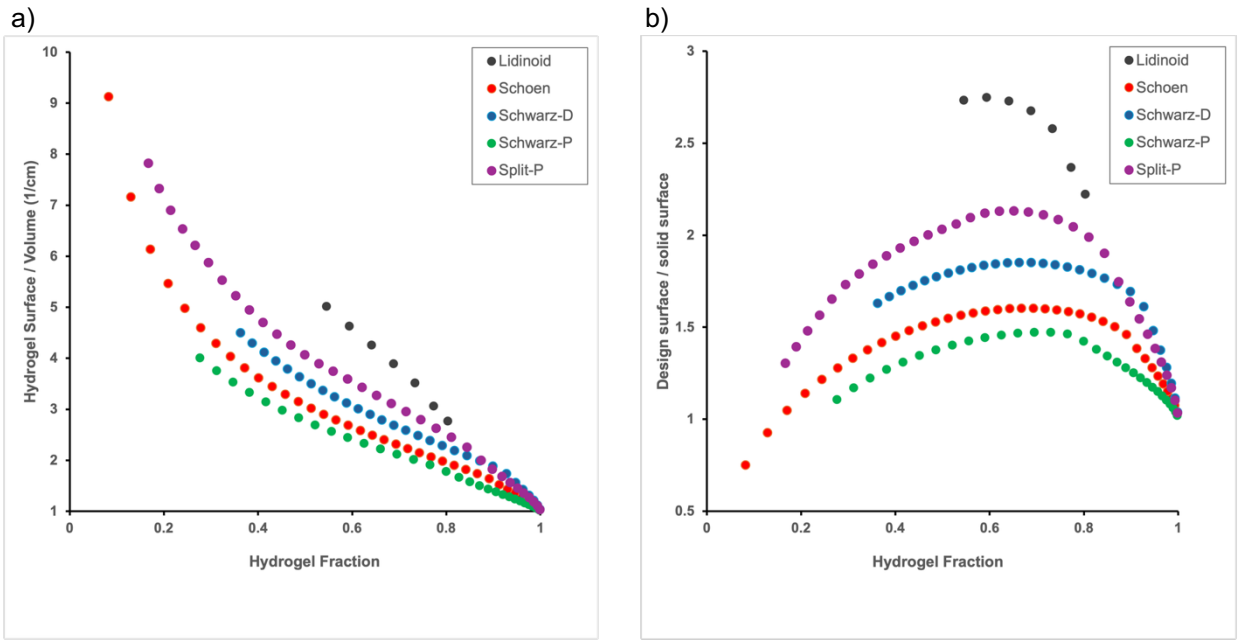

Fig 1

Geometric traits of the TPMS designs considered in this study.
a) Relative surface-area-to-volume ratio (SA/V) *vs*. relative hydrogel fraction (HF) calculated as the hydrogel volume in the design divided by the hydrogel content of a solid cube of the same dimensions. **b)** Relative hydrogel surface area, calculated as the surface area of the design divided by the surface area of a solid cube of the same dimensions, *vs*. the hydrogel fraction (HF).
Only the realisations with HF = 0.6 were 3D printed and tested with plants.

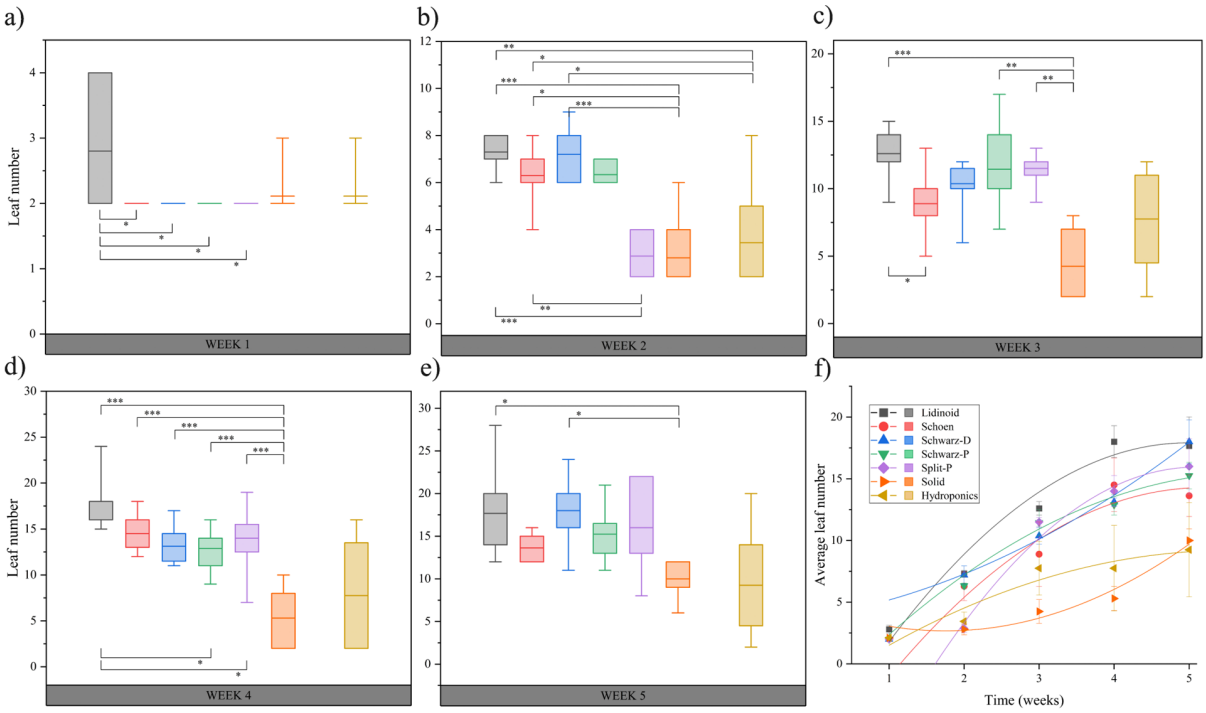

Fig 2

Average number of leaves per plant grown in each substrate design (all realised with HF = 0.6).

a - e) Each box-plot represents the distribution of the plant-average number of leaves across the population of plants grown in that substrate; the lower and upper limits of each box represent the 25th and 75th percentiles of the data, respectively, the whiskers represent the 5th and 95th percentiles, and the horizontal line represents the mean. **f)** Each symbol represents the average leaf number of all plants grown in each substrate, at the corresponding week. Error bars, s.e.m.

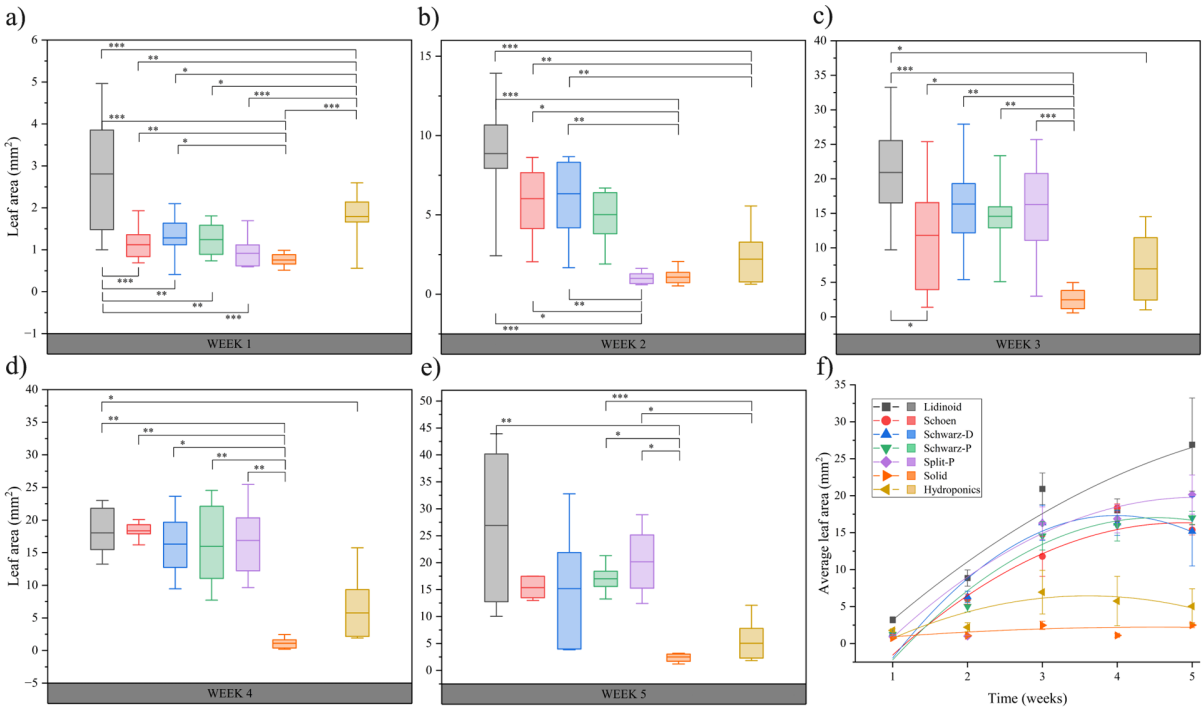

Fig 3.

Average leaf area per plant grown in each substrate design (all realised with HF = 0.6).

a - e) Each box-plot represents the the distribution of the plant-average leaf area across the population of plants grown in that substrate; the lower and upper limits of each box represent the 25th and 75th percentiles of the data, respectively, the whiskers represent the 5th and 95th percentiles, and the horizontal line represents the mean. **f)** Each symbol represents the average leaf area of all plants grown in each substrate, at the corresponding week. Error bars, s.e.m.

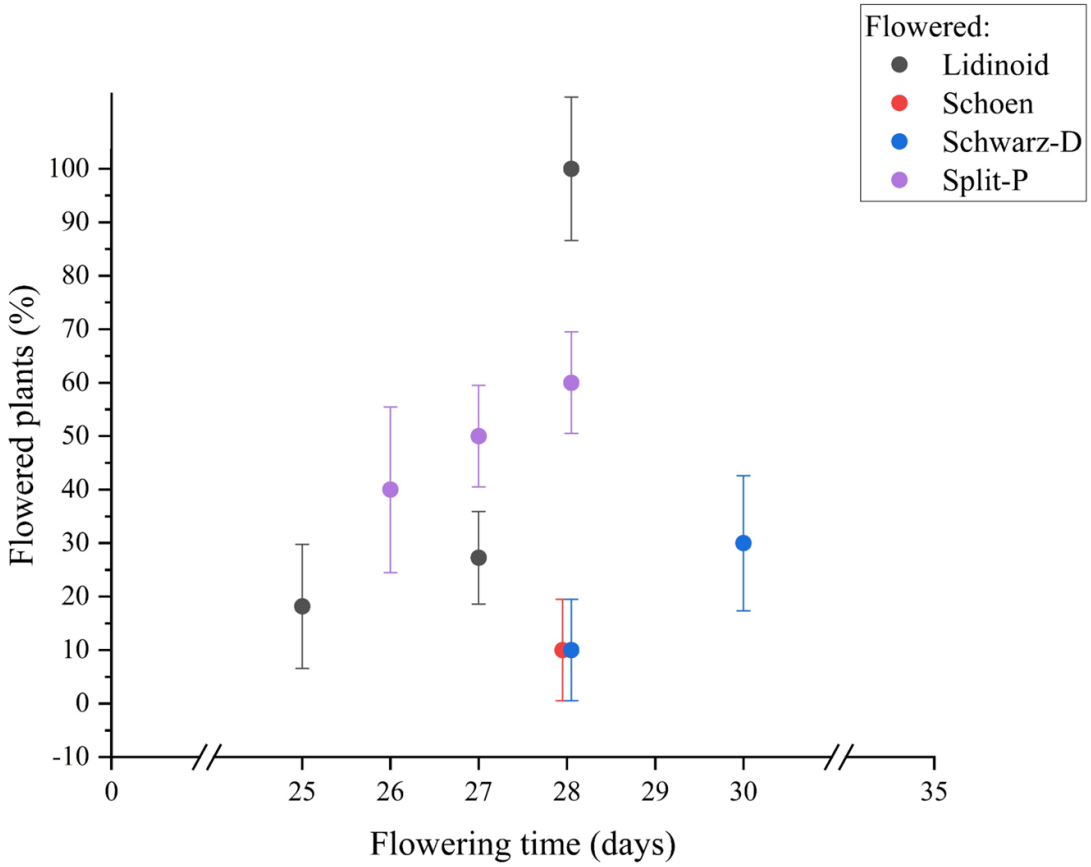

Fig 4.
Percentage of plants flowering each day, when grown in each substrate design (all realised with HF = 0.6) for a total of five weeks (35 days). Plants grown in solid hydrogel, hydroponics and Schwarz-P did not flower in the first 35 days. Error bars, s.e.p.

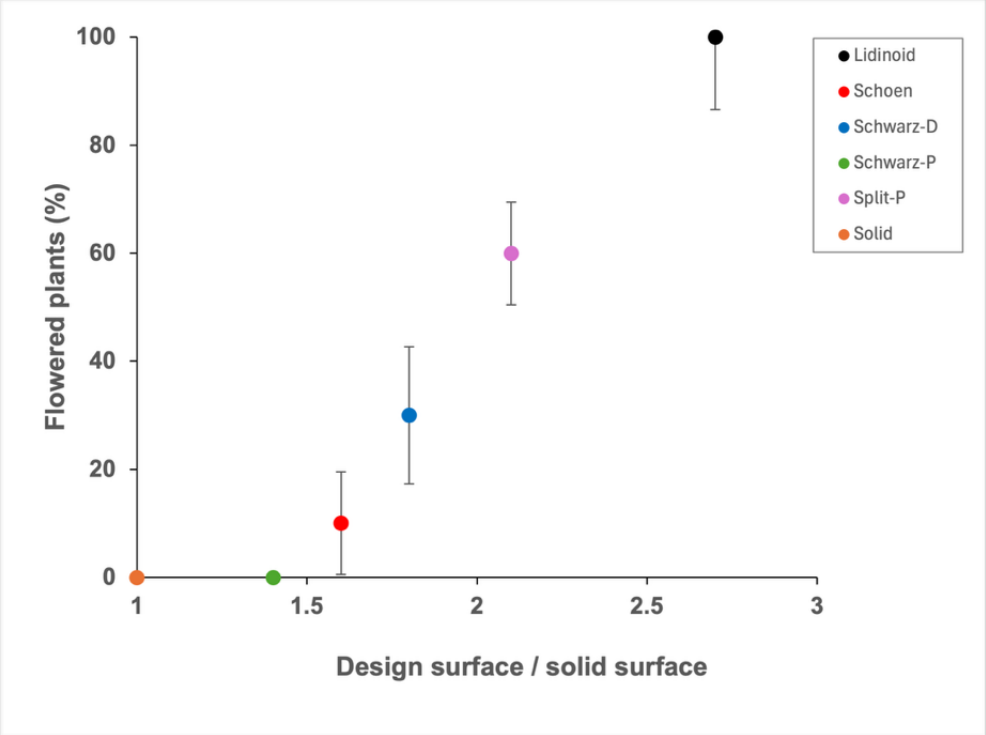

FIG 5

Correlation between the proportion of flowering plants at day 35 and the relative hydrogel surface area of each substrate design (all realised with HF = 0.6), calculated as the surface area of the design divided by the surface area of a solid cube of the same dimensions.

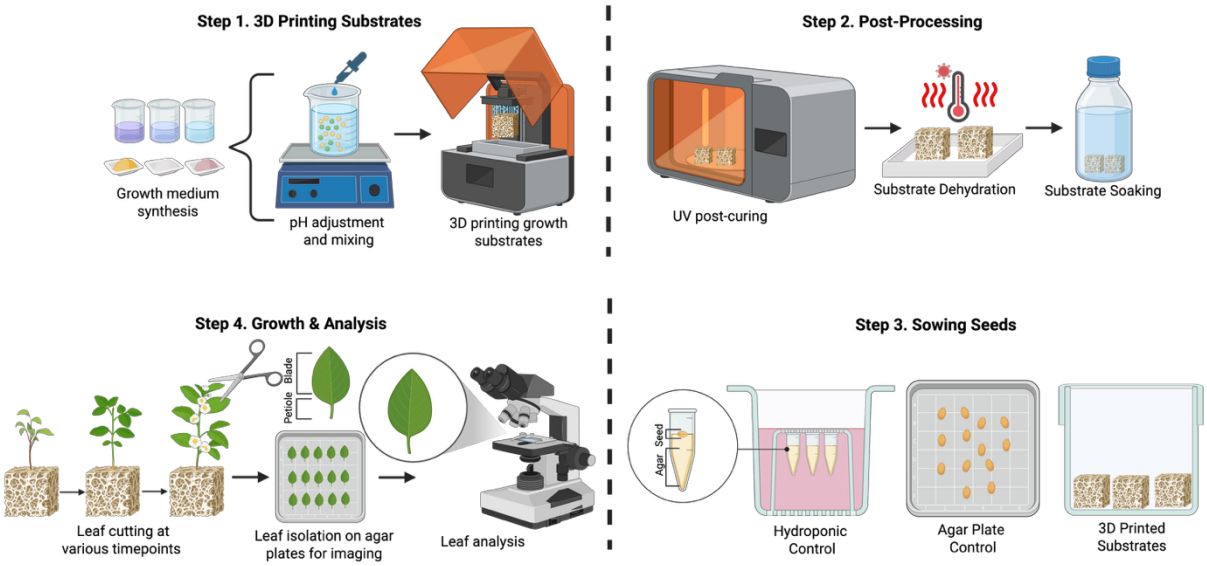

Supplementary Figure 1. Schematic of the experimental pipeline used in this work.

	WEEK 1		WEEK 2		WEEK 3		WEEK 4		WEEK 5	
	Kruskal-Wallis ANOVA	Dunn's test	Kruskal-Wallis ANOVA	Dunn's test	Kruskal-Wallis ANOVA	Dunn's test	One-way ANOVA	Tukey's test	One-way ANOVA	Tukey's test
	P-value	*P*-value	*P*-value	*P*-value	*P*-value	*P*-value	*P*-value	*P*-value	*P*-value	*P*-value
Overall	**0.005**		**4E-07**		**4E-05**		**1E-09**		**0.012**	
Schoen vs lidinoid		**0.018**		1		**0.037**		0.288		0.412
Schwarz-D vs lidinoid		**0.018**		1		0.824		**0.031**		1
Schwarz-D vs schoen		1		1		1		0.945		0.326
Schwarz-P vs lidinoid		**0.018**		1		1		**0.017**		0.860
Schwarz-P vs schoen		1		1		1		0.887		0.960
Schwarz-P vs schwarz-D		1		1		1		1		0.782
Solid vs lidinoid		0.284		**8E-05**		**3E-05**		**0**		**0.020**
Solid vs schoen		1		**0.025**		1		**3E-06**		0.532
Solid vs schwarz-D		1		**3E-04**		0.105		**1E-05**		**0.014**
Solid vs schwarz-P		1		0.164		**0.009**		**1E-05**		0.157
Split-P vs lidinoid		**0.018**		**4E-04**		1		0.117		0.976
Split-P vs schoen		1		0.055		0.653		1		0.868
Split-P vs schwarz-D		1		**0.001**		1		0.990		0.948
Split-P vs schwarz-P		1		0.257		1		0.965		1
Split-P vs solid		1		1		**0.002**		**1E-06**		0.111

Supplementary Table 1. Statistical analysis of leaf number among the 6 hydrogel designs. Statistically significant differences in bold.

	WEEK 1	WEEK 2	WEEK 3	WEEK 4	WEEK 5
	Mann-Whitney test	Mann-Whitney test	Mann-Whitney test	Two-sample *t*-test	Two-sample *t*-test
	P-value	*P*-value	*P*-value	*P*-value	*P*-value
Lidinoid vs hydroponics	0.108	**0.001**	0.022	0.012	0.081
Schoen vs hydroponics	0.947	**0.007**	0.797	0.145	0.336
Schwarz-D vs hydroponics	0.947	**0.002**	0.364	0.220	0.048
Schwarz-P vs hydroponics	0.947	0.014	0.210	0.237	0.215
Solid vs hydroponics	1	0.628	0.190	0.364	0.860
Split-P vs hydroponics	0.947	0.984	0.074	0.061	0.139

Supplementary Table 2. Statistical analysis of leaf number between hydroponics control and 6 hydrogel designs. Bonferroni's correction was applied to all tests. Statistically significant differences in bold.

	WEEK 1		WEEK 2		WEEK 3		WEEK 4		WEEK 5	
	Kruskal-Wallis ANOVA	Dunn's test	Kruskal-Wallis ANOVA	Dunn's test	One-way ANOVA	Tukey's test	Kruskal-Wallis ANOVA	Dunn's test	Kruskal-Wallis ANOVA	Dunn's test
	P-value	*P*-value	*P*-value	*P*-value	*P*-value	*P*-value	*P*-value	*P*-value	*P*-value	*P*-value
Overall	**9E-12**		**2E-07**		**1E-05**		**2E-04**		**0.005**	
Schoen vs lidinoid		**8E-05**		1		**0.037**		1		1
Schwarz-D vs lidinoid		**0.004**		1		0.665		1		1
Schwarz-D vs schoen		1		1		0.695		1		1
Schwarz-P vs lidinoid		**0.003**		0.792		0.280		1		1
Schwarz-P vs schoen		1		1		0.941		1		1
Schwarz-P vs schwarz-D		1		1		0.993		1		1
Solid vs lidinoid		**4E-11**		**1E-05**		**3E-06**		**0.005**		**0.007**
Solid vs schoen		0.156		**0.014**		**0.048**		**0.002**		0.159
Solid vs schwarz-D		**0.008**		**0.005**		**0.001**		**0.010**		0.170
Solid vs schwarz-P		**0.011**		0.284		**0.004**		**0.008**		**0.016**
Split-P vs lidinoid		**9E-09**		**2E-05**		0.594		1		1
Split-P vs schoen		1		**0.017**		0.655		1		1
Split-P vs schwarz-D		0.152		**0.007**		1		1		1
Split-P vs schwarz-P		0.198		0.275		0.992		1		1
Split-P vs solid		1		1		**5E-04**		**0.007**		**0.014**

Supplementary Table 3. Statistical analysis of average leaf area among the 6 hydrogel designs. Statistically significant differences in bold.

	WEEK 1	WEEK 2	WEEK 3	WEEK 4	WEEK 5
	Two-sample *t*-test	Two-sample *t*-test	Two-sample *t*-test	Two-sample *t*-test	Two-sample *t*-test
	P-value	*P*-value	*P*-value	*P*-value	*P*-value
Lidinoid vs hydroponics	**1E-04**	**8E-05**	**0.004**	**0.005**	0.027
Schoen vs hydroponics	**5E-04**	**7E-04**	0.311	0.031	0.018
Schwarz-D vs hydroponics	**0.007**	**7E-04**	0.039	0.009	0.138
Schwarz-P vs hydroponics	**0.004**	0.012	0.051	0.023	**2E-04**
Solid vs hydroponics	**2E-06**	0.104	0.226	0.258	0.362
Split-P vs hydroponics	**2E-05**	0.085	0.034	0.011	**0.004**

Supplementary Table 4. Statistical analysis of average leaf area between hydroponics control and 6 hydrogel designs. Bonferroni's correction was applied to all tests. Statistically significant differences in bold.